J. Phys.: Condens. Matter **20** (2008) 494212 (6pp) doi:10.1088/0953-8984/20/49/494212

Structural transitions in amorphous H_2O and D_2O: the effect of temperature

Katrin Winkel[1], Marion Bauer[1], Erwin Mayer[1], Markus Seidl[2], Michael S Elsaesser[2] and Thomas Loerting[2]

[1] Institute of General, Inorganic and Theoretical Chemistry, University of Innsbruck, Innrain 52a, A-6020 Innsbruck, Austria
[2] Institute of Physical Chemistry, University of Innsbruck, Innrain 52a, A-6020 Innsbruck, Austria

E-mail: thomas.loerting@uibk.ac.at

Received 24 July 2008, in final form 29 September 2008
Published 12 November 2008
Online at stacks.iop.org/JPhysCM/20/494212

Abstract

We have recently observed amorphous–amorphous transitions incurred upon decompressing very high density amorphous ice (VHDA) at 140 K from 1.1 to <0.02 GPa in a piston–cylinder setup by monitoring the piston displacement as a function of pressure and by taking powder x-ray diffractograms of quench-recovered samples (Winkel *et al* 2008 *J. Chem. Phys.* **128** 044510). Here we study the effect of changing the temperature from 77 to 160 K during decompression from 1.1 to <0.02 GPa, and the effect of substituting D_2O for H_2O at 140 and 143 K. At 77 K all structural transitions are arrested and six-coordinated VHDA is quench recovered. At 125–136 K the continuous transition to five-coordinated expanded high density amorphous ice (eHDA) takes place. At 139–140 K, both the continuous transition to eHDA and the quasi-discontinuous transition to four-coordinated LDA are observed, i.e. VHDA → eHDA → LDA. At 142–144 K, crystallization to mixtures of cubic ice Ic and ice IX is observed prior to the quasi-discontinuous transition, i.e. VHDA → eHDA → ice Ic/ice IX. At 160 K ice Ic is recovered, which most likely transforms from a high-pressure ice (HPI) such as ice V, i.e. VHDA → HPI → ice Ic. Exchanging D_2O for H_2O at 140 K does not significantly affect the amorphous–amorphous transitions: both the decompression curves and the powder x-ray diffractograms are unaffected within the experimental resolution. However, at 143 K D_2O–VHDA can be decompressed according to the sequence VHDA → eHDA → LDA, i.e. crystallization can be suppressed at ∼3 K higher temperatures.

1. Introduction

Amorphous ices can be produced by a number of routes such as deposition of water vapour on very cold surfaces [1], hyperquenching of water droplets [2], irradiation of crystalline ice [3, 4] or pressure-induced amorphization of crystalline ice [5]. Whereas amorphous ice is not observed naturally on Earth, it is the most abundant form of ice in space, e.g. on interstellar dust and on comets [6–9]. Three structural states of amorphous ices are known, which are characterized by their density: low density (LDA), high density (HDA) and very high density amorphous ice (VHDA) [10, 11]. All of them are characterized by local tetrahedral order, where one tetrahedron contains a central water molecule and four water molecules are at the four vertices ('Walrafen pentamer') [12, 13]. However, long range order is absent for all amorphous ices. The increase in density from 0.94 g cm^{-3} (LDA) to 1.17 g cm^{-3} (HDA) and 1.26 g cm^{-3} (VHDA) at 77 K and 1 bar [14] is achieved by moving one (HDA) or two (VHDA) molecules from the second hydration shell in LDA to interstitial voids [15–17]. The first hydration shell defined up to a O–O distance of 3.5 Å from a central water molecule contains, therefore, approximately four (LDA), five (HDA) and six (VHDA) water molecules.

Structural transitions between amorphous ices have mainly been investigated by heating the samples stored in liquid nitrogen at ambient pressure [18–28]. Thermal analysis, neutron scattering and T_1-NMR measurements show that both HDA and VHDA transform to LDA at 1 bar when heated to ∼117 ± 3 and ∼126 ± 3 K, respectively [27, 29, 30]. Koza *et al* have established that VHDA transforms at 1 bar to LDA

via a transient, heterogeneous HDA-like state [27, 28]. On further heating, LDA crystallizes to metastable cubic ice Ic at ∼150 K and recrystallizes to the stable hexagonal ice Ih in the range ∼180–220 K [18]. None of these transitions is reversible by cooling the samples again since the Gibbs free energy difference ΔG is negative at 1 bar, i.e. $G(\text{VHDA}) > G(\text{HDA}) > G(\text{LDA}) > G(\text{Ic}) > G(\text{Ih})$. However, with increasing pressure the denser structural states become increasingly favoured. For example, at a pressure of 1.6 GPa the order of stability as defined in terms of Gibbs free energies is reversed, i.e. $G(\text{VHDA}) < G(\text{HDA}) < G(\text{LDA})$. In order to observe 'quasi-equilibrium' structural transitions involving equality of Gibbs free energies, i.e. $\Delta G = 0$, it is necessary to study the structural transitions under *in situ* conditions, i.e. at elevated pressures [31].

Amorphous ices are by definition metastable structural states since an ordered crystalline phase always represents the most stable 'global' minimum. The structural transitions observable in amorphous ices are, therefore, by contrast to structural transitions between stable phases always 'non-equilibrium' transitions [32]. However, if one succeeds in avoiding crystallization it is possible to reach 'quasi-equilibrium' and to switch back and forth between two metastable structural states of equal Gibbs free energy. In view of rapid crystallization of amorphous ices at $T > T_x$ ($T_x \sim 150$ K at 1 bar) this brings the restriction of working at $T < T_x$ for the study of structural transitions in amorphous ices. Such a 'quasi-equilibrium' under *in situ* conditions was first achieved by Mishima *et al* [33, 34], who showed that it is possible to reversibly switch back and forth between LDA and HDA by compressing and decompressing in the temperature range $T \sim 130$–140 K. Since this transition is, in addition to being reversible, very sharp (as observed by a sudden density change) and involves hysteresis the term 'quasi-first-order transition' between amorphous ices was used—this is an entirely new concept in thermodynamics [34]. In order to be legitimately called a 'quasi-first-order transition' the change in order parameter, e.g. density, has to be discontinuous. Such a discontinuous change is consistent with Mishima's experiment [34]. However, it is experimentally very hard, if not impossible, to clearly distinguish a discontinuous transition from a sharp, but continuous transition [10]. Therefore, an uncertainty remains as to whether the LDA ↔ HDA transition is indeed like a first-order transition. A first-order transition is characterized by phase co-existence under suitable p, T conditions and by a reversible latent heat effect. Similarly, a 'quasi-first-order transition' is characterized by 'quasi-phase' co-existence under suitable p, T conditions and by a reversible latent heat effect. Using the technique of *in situ* neutron diffraction Klotz *et al* have inferred that their observed structure factors at $p \sim 0.3$ GPa and $T \sim 130$ K can only be explained as arising from a co-existing mixture of HDA and LDA, but not from a single amorphous structural state [35]. It has been doubted, though, whether the conclusion of HDA–LDA co-existence can be made based on the use of neutrons, and the use of x-rays was suggested instead [36]. Nelmes *et al* have shown that the HDA-state in quasi-equilibrium with LDA is not identical with the HDA-state obtained by pressure-induced amorphization of hexagonal ice at 77 K and suggested the use of the terminology 'expanded HDA' (eHDA) for the former and 'unrelaxed HDA' (uHDA) for the latter [37].

We have recently studied structural transitions in amorphous ices by compressing LDA at 125 K [38, 39] and by decompressing VHDA at 140 K [40] using a piston–cylinder setup. The *in situ* structural states were kinetically arrested by quenching to liquid nitrogen temperature and by slowly releasing the pressure and subsequently investigated by Cu Kα powder x-ray diffraction. We have found two structural transitions. First, a sharp, apparently discontinuous and reversible transition between LDA and eHDA in accordance with the results presented by Mishima [34]. In addition we observe *both* eHDA *and* LDA upon decompression of VHDA at $T \sim 140$ K to $p \sim 0.06$ GPa by x-ray diffraction, but no structural states in between [40]. This x-ray result is consistent with 'quasi-phase co-existence' between LDA and eHDA as also suggested by Klotz *et al* from *in situ* neutron diffraction [35] and Yoshimura *et al* from *in situ* diamond anvil cell Raman studies [41]. Second, we have found a less sharp and continuous transition between VHDA and eHDA, which takes place in the pressure range $p \sim 0.07$–0.40 GPa upon decompression at $T \sim 140$ K [40] and in the pressure range $p \sim 0.80$–1.00 GPa [38, 39] upon compression at $T \sim 125$ K. A large, if not infinite, number of structural states between VHDA and eHDA can be prepared, whereas not a single structural state between eHDA and LDA was observed. Hemley *et al* and Klotz *et al* have shown that upon continued compression of VHDA no further structural changes are observable until it crystallizes to orientationally disordered ice VII at 4 GPa and 77 K [42, 43]. Therefore, eHDA and VHDA are the end members of a continuous structural transition, which in a sense resembles a second-order transition showing a density kink [44].

Here we study the effect of temperature variation and the effect of exchanging D_2O for H_2O on the decompression of VHDA.

2. Experimental details

H_2O–VHDA and D_2O–VHDA are prepared using the standard technique employed also for earlier studies [14, 39, 40, 45]. In brief, 300 μl of doubly distilled, deionized H_2O or 300 μl of D_2O (Fluka, >99.8%) are pipetted into the 8 mm bore of a hardened steel cylinder, which is cooled to 77 K by immersion in liquid nitrogen and lined with a cup made of ∼300 mg of thin indium foil, which serves as a low-temperature lubricant. Temperature is measured using a Pt-100 sensor counter-sunk in the steel cylinder, which is sitting at a distance of about 10 mm from the sample. The hexagonal ice, which freezes within the cup, is then pressurized by moving a piston slowly down the bore. When the pressure exceeds $p \sim 1.0$ GPa the hexagonal ice amorphizes and forms 'unrelaxed HDA' (uHDA) [5, 37]. The use of the indium cup ensures that the pressure builds up according to the programmed compression rate and avoids release of uncontrolled shock-waves, which have the potential of transforming the sample to unwanted ice XII [46–50]. uHDA is subsequently transformed to VHDA by pressure-

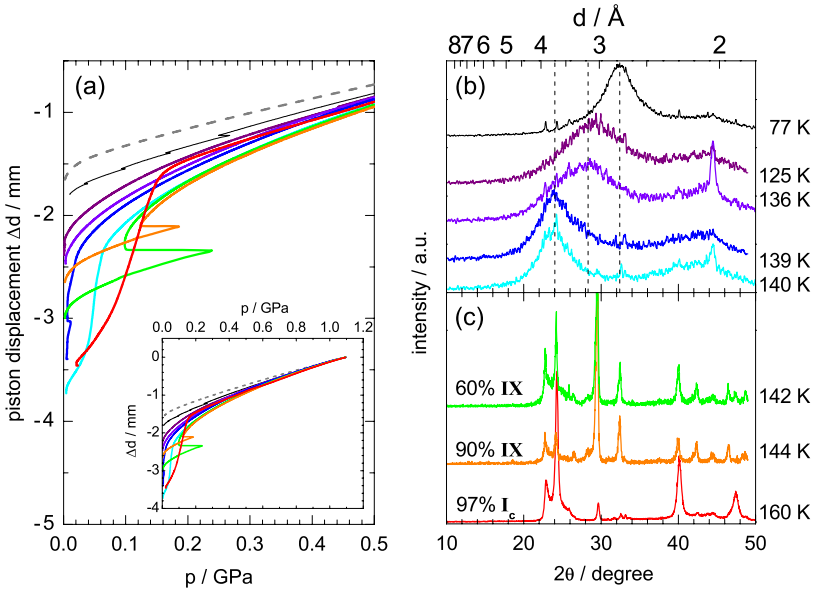

Figure 1. (a) Evolution of the piston displacement, Δd, as a function of the nominal pressure, p, upon decompression of 300 mg H_2O VHDA from 1.1 GPa to <0.02 GPa at a rate of 20 MPa min^{-1} in a cylinder with an 8 mm bore. The samples are lined with 300 mg of thin indium foil for reducing friction at low temperatures. Eight traces recorded at different constant temperatures are shown and distinguished by means of their colour: black (77 K), purple (125 K), violet (136 K), blue (139 K), turquoise (140 K), green (142 K), orange (144 K) and red (160 K). The dashed trace corresponds to a blind experiment done without a VHDA sample at 77 K. The inset shows the whole decompression curve, the main panel shows a magnified pressure range from 0.0 to 0.5 GPa. The curve recorded at 140 K is identical to the curve shown in figure 2 and marked (11) in Winkel *et al* [40]). (b)/(c) x-ray diffraction patterns for the eight samples after the decompression procedure, which were recovered and stored in liquid nitrogen and measured in θ–θ geometry using an incident wavelength of 1.54 Å (Cu Kα) at $T \sim 83$ K. (b) shows amorphous diffraction patterns characterized by an intense first broad diffraction maximum in the range $2\theta \sim 24.0°$–$32.3°$ and a less intense second broad maximum at $2\theta > 40°$. The dashed vertical lines mark the position of the intense broad maximum for LDA at $2\theta \sim 24.0°$, eHDA at $2\theta \sim 28.3°$ and VHDA at $2\theta \sim 32.3°$. Tiny sharp Bragg reflections at $2\theta \sim 22°$, 24°, 26°, 40° and 46° arise from hexagonal ice, which condenses on the surface of the x-ray amorphous samples upon transferring the sample from liquid nitrogen to the sample holder. Additional Bragg reflections at $2\theta \sim 30°$, 33° and $2\theta \sim 44°$ may arise from small remnants of indium or the sample holder made of chrome-plated copper. (c) shows crystalline diffraction patterns characterized by sharp Bragg reflections. The green and orange traces, corresponding to decompression temperatures of 142 and 144 K are identified as 6:4 and 9:1 mixtures of the high-pressure polymorph ice IX and cubic ice Ic, respectively. Mixing ratios were estimated by using the program Powder Cell (see text). The red trace, corresponding to a decompression temperature of 160 K is identified as 97% cubic ice.

annealing the sample at $p \sim 1.1$ GPa to $T \sim 160$ K [14]. Next, the sample is brought to the desired temperature while keeping the pressure constant at 1.1 GPa. In the case of H_2O, we have studied samples at 77, 125, 136, 139, 140, 142, 144 and 160 K (cf figure 1), in the case of D_2O we have studied samples at 140 and 143 K (cf figure 2). Usually the temperature as read out by the Pt-100 sensor shows a standard deviation of no more than ±0.2 K [56]. Finally, the sample is decompressed at a controlled rate of 20 MPa min^{-1} at constant temperature to <0.02 GPa and recovered by immersing in liquid nitrogen and pushing out of the cylinder. The decompression run takes about an hour. The diffractograms (Cu Kα) of the recovered samples were recorded at ~83 K on a diffractometer in Θ–Θ geometry (Siemens, model D 5000), equipped with a low-temperature camera of Anton Paar. In some 'amorphous' powder diffractograms, sharp features can be seen. They arise from traces of hexagonal ice Ih, which had formed by condensation of water vapour during transfer of the sample onto the precooled sample holder [51], e.g. figure 2, (D1) and (H8), or the x-ray sample holder itself (chrome-plated Cu: $2\Theta = 44.5°$), e.g. figure 1(b), 136 and 140 K. The samples themselves are fully amorphous.

3. Results

In figure 1(a) the decompression curves of H_2O–VHDA are shown for eight temperatures. It can immediately be seen that change of temperature has a tremendous effect, especially in the pressure range $p < 0.3$ GPa. Therefore, the whole pressure range is shown as an inset, and the pressure range $0.00 < p < 0.50$ GPa is shown in magnification. The ordinate (y-axis) in fig 1(a) shows the piston displacement as measured directly by the material testing machine. The final position of the piston at the end of the decompression run varies between −1.8 mm (77 K) and −3.7 mm (140 K). This piston position approximately correlates with sample density according to the formula given in [39], so that −1.8 mm corresponds to roughly 1.26 g cm^{-3} and −3.7 mm corresponds to roughly 0.94 g cm^{-3}. That is, the VHDA decompression procedure produces samples in the density range $\rho \sim 0.94$–1.26 g cm^{-3}.

The 77 K curve (figure 1(a), black trace) falls slightly below the blind experiment recorded without pipetting a sample into the indium cup (figure 1(a), dashed line), which reflects the fact that the isothermal compressibility of VHDA is higher than the apparatus compressibility. That is, by decompressing VHDA slowly at 77 K merely elastic reduction

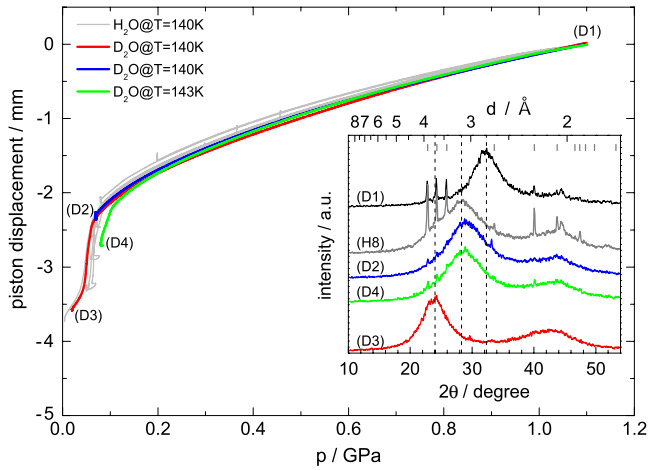

Figure 2. Evolution of the piston displacement, Δd, as a function of the nominal pressure, p, upon decompression of 300 mg D_2O VHDA from 1.1 GPa to <0.02 GPa at a rate of 20 MPa min^{-1} in a cylinder with an 8 mm bore. The samples are lined with 300 mg of thin indium foil for reducing friction at low temperatures. The blue and red traces were recorded at 140 K, the green trace at 143 K. The light-grey traces correspond to the set of H_2O traces recorded at 140 K and shown in figure 2 in Winkel *et al* [40]. The inset shows the powder x-ray diffractograms recorded after recovering the samples from the marks (D1), (D2), (D3) and (D4) in liquid nitrogen. For comparison the light-grey powder diffractogram marked (H8) is taken from figure 3(a), trace 8 in Winkel *et al* [40] and corresponds to H_2O–VHDA decompressed to 0.07 GPa at 140 K. The dashed vertical lines mark the position of the intense broad maximum for LDA at $2\theta \sim 24.0°$, eHDA at $2\theta \sim 28.3°$ and VHDA at $2\theta \sim 32.3°$.

of the density from ∼1.36 g cm^{-3} at 1 GPa to ∼1.26 g cm^{-3} at 1 bar [38], but no structural transition takes place. The structural state observed by powder x-ray diffraction after decompressing VHDA at 77 K is still VHDA. In other words, by recovering VHDA (and also other amorphous structural states) from *in situ* conditions to 1 bar at 77 K, one has the opportunity to study a kinetically arrested high-pressure state at 1 bar.

By contrast, both at 125 and 136 K (figure 1(a), purple and violet traces) the decompression curves deviate more strongly and in a nonlinear fashion from the blind experiment below $p \sim 0.3 \pm 0.1$ GPa and show a final piston position of -2.4 ± 0.1 mm, which roughly corresponds to a density of 1.14 ± 0.03 g cm^{-3}. The powder x-ray diffractograms for these two quench-recovered samples still show the broad halos characteristic of amorphous states. A shift in the first broad maximum from $2\theta \sim 32.3°$ in VHDA to $2\theta \sim 28.3°$ (violet trace) indicates that a structural transition has occurred along the decompression path to a state, which can best be described as 'expanded HDA' (eHDA). The eHDA diffraction pattern from [40] (figure 3, trace 8) is reproduced here in figure 2 as trace (H8) for comparison.

At 139 and 140 K (figure 1(a), blue and turquoise traces) in addition to the continuous transition VHDA → eHDA, a sharp and large drop in the piston displacement to a final position of −3.4 mm (∼0.96 g cm^{-3}) and −3.7 mm (∼0.94 g cm^{-3}) is observed starting at 0.04 ± 0.01 and 0.07 ± 0.01 GPa, respectively. This corresponds to the quasi-discontinuous transition eHDA → LDA [40]. It is interesting to note that a temperature difference of just 1 K results in a quite significant change of the pressure, where the quasi-discontinuous transition takes place. The diffractograms of the quench-recovered samples shown in figure 1(b) show the amorphous powder pattern typical of LDA with the maximum of the first halo peak at $2\theta \sim 24.0°$. The turquoise diffractogram (140 K) shows pure LDA. A slight asymmetry on the high angle side is indicative of a few per cent of eHDA in the blue diffractogram (139 K), which have not converted to LDA. The full width at half maximum (FWHM) is increased from 4.6° (pure LDA, 140 K) to 5.6° (139 K). Judging from the density, the amount of unconverted eHDA is about 5–10% (139 K).

At 142 K (figure 1(a), green trace) the decompression curve closely follows the 140 K curve down to ∼0.2 GPa. At $p \sim 0.10$ GPa, where eHDA should have already formed, a sudden event takes place, which causes a sudden volume increase (density decrease). This event is so rapid that the material testing machine is unable to raise the piston quickly enough, and hence the pressure increases for a moment to ∼0.24 GPa, before the programmed decompression routine continues. The powder x-ray diffractogram in figure 1(c) of the recovered sample shows Bragg peaks characteristic for a mixture of ice IX and ice Ic, and so the sudden event can be attributed to crystallization. Using the published crystal structures for ice IX and ice Ic [52] and the program 'Powder Cell' [53], we calculate a fraction of 60% ice IX and 40% ice Ic. Given a density of 1.16 g cm^{-3} for ice IX and 0.93 g cm^{-3} for ice Ic [52] this mixture would have a density of 1.07 g cm^{-3}, which is consistent with the final piston position. Similarly, at 144 K (figure 1(a), orange trace) the curve closely follows the 140 K curve down to ∼0.2 GPa and then deviates from it. At ∼0.12 GPa a sudden event characterized by a slightly lower increase in pressure takes place. Again, this event is found to be crystallization when looking at the powder pattern in figure 1(c). In this case a 90:10 mixture of ice IX and ice Ic is estimated from 'Powder Cell'. The estimated density of 1.14 g cm^{-3} is again consistent with the final piston position.

At 160 K the decompression curve (figure 1(a), red trace) follows the curve at 144 K closely down to ∼0.5 GPa and then shows a slope different from most other curves. Looking at the crystallization line T_x (e.g. figure 8 in [51]) one finds that HDA crystallizes at 160 K at pressures below about 0.7 ± 0.1 GPa. Therefore, it is likely that VHDA crystallizes at 160 K when decompressing to below 0.7 GPa. Surprisingly, no sudden change in density can be observed in the pressure range $p \sim$ 0.2–1.1 GPa in the decompression curve. This implies that VHDA either does not crystallize in this pressure range, which we regard as unlikely, or it crystallizes to a phase of equal density under high pressure[3], which could possibly be ice V or another high-pressure polymorph of ice [51]. We regard the latter scenario as more likely. At a pressure of ∼0.15 GPa a sharp drop in piston displacement to a final piston position of −3.5 mm (∼0.94 g cm^{-3}) indicates a transition to a less

[3] Also LDA crystallizes to a phase of equal density, namely to ice Ic at low pressures. The LDA → Ic transition can thus not be located in piston displacement versus temperature plots.

dense phase. According to the powder x-ray diffractogram in figure 1(c) this phase is 97% cubic ice Ic with a trace of ice IX. The trace of ice IX survives at 160 K and 0.02 GPa (200 bar), but transforms to ice Ic at 160 K and ambient pressure (1 bar). We assume the sharp change in piston position to be due to ice recrystallization rather than crystallization of amorphous ice.

In figure 2 we show decompression curves for D_2O–VHDA at temperatures of 140 and 143 K together with the quench-recovered powder diffractograms as an inset. The light-grey curves are reproduced from figure 2 in [40] and show the decompression curves of H_2O–VHDA at a temperature of 140 K. The light-grey diffractogram in the inset shows H_2O–eHDA as obtained by decompression to 0.07 GPa. The full D_2O-decompression run (figure 2, red trace) cannot be distinguished from the full H_2O-decompression run (figure 2, light-grey trace). As for the H_2O case, the onset of the sharp transition is found at 0.07 ± 0.01 GPa in the D_2O case at 140 K, and the final piston position is almost identical for H_2O and D_2O. Also the powder diffractograms of D_2O–VHDA (figure 2, inset (D1)), D_2O–eHDA (figure 2, inset (D2)) and D_2O–LDA (figure 2, inset (D3)) can hardly be distinguished from H_2O–VHDA (figure 1(b), black trace, 77 K), H_2O–eHDA (figure 2, inset (H8)) and H_2O–LDA (figure 1(b), turquoise trace, 140 K), respectively. That is, at 140 K just a marginal difference within the experimental resolution can be identified for D_2O–VHDA versus H_2O–VHDA decompression. However, at 143 K (figure 2, green curve) eHDA can be produced by decompressing to 0.08 GPa without crystallization. Also LDA can be produced by fully decompressing at 143 K (curve not shown), i.e. the transition sequence VHDA $\rightarrow$ eHDA $\rightarrow$ LDA can be observed. At slightly higher temperatures, e.g. 144 K, we have also observed crystallization in D_2O (curves not shown), so that crystallization is suppressed in the temperature range 141–143 K when using D_2O instead of H_2O.

4. Discussion and conclusions

In conclusion we have shown that the temperature is an important parameter in governing structural transitions upon decompressing very high density amorphous ice (H_2O–VHDA). Whereas at 77 K structural transitions can be effectively suppressed, structural amorphous–amorphous transitions take place in the range 125–140 K and crystallization takes place at $T > 140$ K.

The transition to LDA can be suppressed by working at $T < 137$ K, whereas the transition sequence VHDA $\rightarrow$ eHDA $\rightarrow$ LDA is observed merely in the narrow temperature interval $T \sim 139$–140 K. The same amorphous–amorphous transitions can be observed in D_2O–VHDA at 140 K. Interestingly, the amorphous–amorphous transitions are not shifted to different pressures compared to H_2O, whereas crystallization takes place at slightly higher temperatures ($\sim$3 K), i.e. crystallization in VHDA can be avoided up to 143 K in D_2O but only up to 140 K in H_2O. It is not unusual that phase transitions are shifted to slightly higher temperatures in D_2O as compared to H_2O, e.g. D_2O ice melts at 277 K rather than 273 K. The close agreement between D_2O–VHDA and H_2O–VHDA decompression at 140 K implies that under identical p, T conditions, the structural states of D_2O and H_2O amorphous ices will be the same, i.e. the technique of isotope substitution neutron diffraction [17] can be successful in obtaining structural models of the states along the VHDA decompression path.

The 'opportunity' to study quench-recovered states at 77 K and 1 bar, which are structurally analogous to the high-pressure states, is in reality a necessary condition if one wants to make a judgement on the nature of high-pressure structural transitions by studying powder x-ray diffractograms, vibrational spectra, thermal properties etc at 1 bar. Klotz *et al* have shown that the elastic change in density upon changing pressure is mainly achieved by contracting/expanding the OO-coordination shells even as high as 100 K, whereas the OD- and DD-correlation functions are barely affected by change in pressure [54]. That is, quench-recovery of amorphous ices results in a kinetically arrested state when done at temperatures not higher than 100 K.

At higher temperatures, in the range 125–140 K, structural amorphous–amorphous transitions take place. eHDA is produced at the low-pressure end upon decompressing VHDA at 125–136 K, whereas LDA is produced at 139–140 K. Isotope substitution neutron diffraction measurements indicate that both eHDA and LDA show significant structural differences from VHDA, which are evident in all partial correlation functions, i.e. $g_{OO}(r)$, $g_{OH}(r)$ and $g_{HH}(r)$ [15–17, 55]. As outlined in the introduction, two interstitial water molecules need to move to the second hydration shell for the downstroke conversion of VHDA to LDA. The first of the two interstitial water molecules starts to move toward the second hydration shell at $p \sim 0.3 \pm 0.1$ GPa and $T \sim 125$ K and 'slowly moves' until it completes its movement at pressures close to ambient. This is consistent with a decompression curve, which slowly deviates from the 77 K experiment (figure 1(a), black trace) at $p < 0.3$ GPa and by the powder diffractograms showing the first halo peak between the eHDA and VHDA halo peaks [40]. By contrast, the second interstitial water molecule remains in its position down to 0.04 ± 0.01 GPa (139 K, H_2O), 0.07 ± 0.01 GPa (140 K, H_2O and D_2O) and 0.10 ± 0.01 GPa (143 K, D_2O) and then suddenly 'jumps' to the second hydration shell. This is consistent with the sharp change in piston displacement and the sudden shift of the first halo peak from eHDA to LDA, with no intermediate halo peaks observed either in D_2O (reported here) or H_2O (reported in [40]).

At slightly higher temperatures, rapid crystallization sets in since the crystallization line is crossed, e.g. at 0.10 GPa and 142 K (H_2O) or 0.12 GPa and 144 K (H_2O). Judging from the piston position prior to crystallization it seems that eHDA forms prior to crystallization. Mixtures of ice IX and ice Ic are observed as the crystallization product from presumably eHDA. Previously, it was shown that mixtures of ice Ih and ice IX crystallize upon isobaric heating of HDA at 0.21 GPa [51] and mixtures of ice II and ice III/IX crystallize upon compressing ice Ih beyond 0.2–0.3 GPa [56]. At higher temperatures such as 160 K VHDA very likely crystallizes directly to a high-pressure ice polymorph such as ice V and

recrystallizes subsequently upon continued decompression to cubic ice Ic. The transition to the high-pressure polymorph, however, cannot be observed by monitoring the piston displacement. We assume this is because of incidentally equal densities of the high-pressure polymorph and VHDA.

Acknowledgments

We are grateful to the Austrian Science Fund (FWF, grants no. R37-N11 and Y391) and the European Research Council (ERC starting grant SULIWA) for supporting this work and to Daniel T Bowron, John L Finney, G Franzese and Philip S Salmon for helpful discussions.

References

[1] Burton E F and Oliver W F 1935 *Nature* **135** 505
[2] Mayer E 1985 *J. Appl. Phys.* **58** 663
[3] Kouchi A and Kuroda T 1990 *Nature* **344** 134
[4] Leto G and Baratta G A 2003 *Astron. Astrophys.* **397** 7
[5] Mishima O, Calvert L D and Whalley E 1984 *Nature* **310** 393
[6] Smoluchowski R 1981 *Astrophys. J.* **244** L31
[7] Kouchi A and Yamamoto T 1995 *Prog. Cryst. Growth Charact. Mater.* **30** 83
[8] Jenniskens P, Blake D F, Wilson M A and Pohorille A 1995 *Astrophys. J.* **455** 389
[9] Baragiola R A 2003 *Planet. Space Sci.* **51** 953
[10] Debenedetti P G 2003 *J. Phys.: Condens. Matter* **15** R1669
[11] Loerting T and Giovambattista N 2006 *J. Phys.: Condens. Matter* **18** R919
[12] Walrafen G E 1964 *J. Chem. Phys.* **40** 3249
[13] Walrafen G E 1967 *J. Chem. Phys.* **47** 114
[14] Loerting T, Salzmann C, Kohl I, Mayer E and Hallbrucker A 2001 *Phys. Chem. Chem. Phys.* **3** 5355
[15] Finney J L, Hallbrucker A, Kohl I, Soper A K and Bowron D T 2002 *Phys. Rev. Lett.* **88** 225503
[16] Finney J L, Bowron D T, Soper A K, Loerting T, Mayer E and Hallbrucker A 2002 *Phys. Rev. Lett.* **89** 205503
[17] Bowron D T, Finney J L, Hallbrucker A, Kohl I, Loerting T, Mayer E and Soper A K 2006 *J. Chem. Phys.* **125** 194502
[18] Handa Y P, Mishima O and Whalley E 1986 *J. Chem. Phys.* **84** 2766
[19] Klug D D, Mishima O and Whalley E 1986 *Physica B+C (Amsterdam)* **139/140** 475
[20] Kolesnikov A I, Sinitsyn V V, Ponyatovsky E G, Natkaniec I, Smirnov L S and Li J C 1997 *J. Phys. Chem.* B **101** 6082
[21] Klug D D, Tulk C A, Svensson E C and Loong C K 1999 *Phys. Rev. Lett.* **83** 2584
[22] Mishima O and Suzuki Y 2002 *Nature* **419** 599
[23] Tulk C A, Benmore C J, Urquidi J, Klug D D, Neuefeind J, Tomberli B and Egelstaff P A 2002 *Science* **297** 1320
[24] Guthrie M, Urquidi J, Tulk C A, Benmore C J, Klug D D and Neuefeind J 2003 *Phys. Rev.* B **68** 184110
[25] Gromnitskaya E L, Stal'gorova O V, Lyapin A G, Brazhkin V V and Tarutin O B 2003 *JETP Lett.* **78** 488
[26] Koza M M, Schober H, Fischer H E, Hansen T and Fujara F 2003 *J. Phys.: Condens. Matter* **15** 321
[27] Koza M M, Geil B, Winkel K, Koehler C, Czeschka F, Scheuermann M, Schober H and Hansen T 2005 *Phys. Rev. Lett.* **94** 125506
[28] Koza M M, Hansen T, May R P and Schober H 2006 *J. Non-Cryst. Solids* **352** 4988
[29] Mishima O 1996 *Nature* **384** 546
[30] Scheuermann M, Geil B, Winkel K and Fujara F 2006 *J. Chem. Phys.* **124** 224503
[31] Brazhkin V V 2006 *J. Phys.: Condens. Matter* **18** 9643
[32] McMillan P F 2004 *J. Mater. Chem.* **14** 1506
[33] Mishima O, Calvert L D and Whalley E 1985 *Nature* **314** 76
[34] Mishima O 1994 *J. Chem. Phys.* **100** 5910
[35] Klotz S, Straessle T, Nelmes R J, Loveday J S, Hamel G, Rousse G, Canny B, Chervin J C and Saitta A M 2005 *Phys. Rev. Lett.* **94** 025506
[36] Tulk C A, Benmore C J, Klug D D and Neuefeind J 2006 *Phys. Rev. Lett.* **96** 149601
[37] Nelmes R J, Loveday J S, Straessle T, Bull C L, Guthrie M, Hamel G and Klotz S 2006 *Nat. Phys.* **2** 414
[38] Loerting T, Schustereder W, Winkel K, Salzmann C G, Kohl I and Mayer E 2006 *Phys. Rev. Lett.* **96** 025702
[39] Winkel K, Schustereder W, Kohl I, Salzmann C G, Mayer E and Loerting T 2007 *Proc. 11th Int. Conf. on the Physics and Chemistry of Ice* ed W F Kuhs (Dorchester: RSC) p 641
[40] Winkel K, Elsaesser M S, Mayer E and Loerting T 2008 *J. Chem. Phys.* **128** 044510
[41] Yoshimura Y, Stewart S T, Mao H-K and Hemley R J 2007 *J. Chem. Phys.* **126** 174505
[42] Hemley R J, Chen L C and Mao H K 1989 *Nature* **338** 638
[43] Klotz S, Hamel G, Loveday J S, Nelmes R J and Guthrie M 2003 *Z. Kristallogr.* **218** 117
[44] Salzmann C G, Loerting T, Klotz S, Mirwald P W, Hallbrucker A and Mayer E 2006 *Phys. Chem. Chem. Phys.* **8** 386
[45] Loerting T, Winkel K, Salzmann C G and Mayer E 2006 *Phys. Chem. Chem. Phys.* **8** 2810
[46] Lobban C, Finney J L and Kuhs W F 1998 *Nature* **391** 268
[47] Koza M, Schober H, Tölle A, Fujara F and Hansen T 1999 *Nature* **397** 660
[48] Koza M M, Schober H, Hansen T, Tölle A and Fujara F 2000 *Phys. Rev. Lett.* **84** 4112
[49] Kohl I, Mayer E and Hallbrucker A 2001 *Phys. Chem. Chem. Phys.* **3** 602
[50] Kohl I, Loerting T, Salzmann C, Mayer E and Hallbrucker A 2002 *New Kinds of Phase Transitions: Transformations in Disordered Substances* ed V V Brazhkin *et al* (Amsterdam: Kluwer) p 325
[51] Salzmann C G, Mayer E and Hallbrucker A 2004 *Phys. Chem. Chem. Phys.* **6** 5156
[52] Petrenko V F and Whitworth R W 1999 *Physics of Ice* (Oxford: Oxford University Press)
[53] Kraus W and Nolze G 1996 *J. Appl. Crystallogr.* **29** 301
[54] Klotz S, Straessle T, Saitta A M, Rousse G, Hamel G, Nelmes R J, Loveday J S and Guthrie M 2005 *J. Phys.: Condens. Matter* **17** S967
[55] Bowron D T, Finney J L, Winkel K, Mayer E, Loerting T and Soper A K 2008 in preparation
[56] Bauer M, Elsaesser M S, Winkel K, Mayer E and Loerting T 2008 *Phys. Rev.* B **77** 220105